Thin Solid Films 552 (2014) 136–140

Contents lists available at ScienceDirect

Thin Solid Films

journal homepage: www.elsevier.com/locate/tsf

Molecular dynamics simulation for the influence of incident angles of energetic carbon atoms on the structure and properties of diamond-like carbon films

Xiaowei Li [a], Peiling Ke [a], Kwang-Ryeol Lee [b], Aiying Wang [a,*]

[a] Key Laboratory of Marine Materials and Related Technologies, Zhejiang Key Laboratory of Marine Materials and Protective Technologies, Ningbo Institute of Materials Technology and Engineering, Chinese Academy of Sciences, Ningbo 315201, PR China
[b] Computational Science Research Center, Korea Institute of Science and Technology, Seoul 136–791, South Korea

ARTICLE INFO

Article history:
Received 14 May 2013
Received in revised form 26 November 2013
Accepted 6 December 2013
Available online 14 December 2013

Keywords:
Diamond-like carbon
Residual stress
Incident angles
Molecular dynamics simulation

ABSTRACT

The influence of incident angles of energetic carbon atoms (0–60°) on the structure and properties of diamond-like carbon (DLC) films was investigated by the molecular dynamics simulation using a Tersoff interatomic potential. The present simulation revealed that as the incident angles increased from 0 to 60°, the surface roughness of DLC films increased and the more porous structure was generated. Along the growth direction of DLC films, the whole system could be divided into four regions including substrate region, transition region, stable region and surface region except the case at the incident angle of 60°. When the incident angle was 45°, the residual stress was significantly reduced by 12% with little deterioration of mechanical behavior. The further structure analysis using both the bond angles and bond length distributions indicated that the compressive stress reduction mainly resulted from the relaxation of highly distorted C–C bond length.

1. Introduction

Owning to high hardness, low coefficient of friction, superior optical property, chemical inertness and good biocompatibility, diamond-like carbon (DLC) films are not only widely used as a protective coating in the industrial fields of cutting tools, molds, data storage and so on [1,2], but also considered as a strong candidate for the biomedical applications such as heart valves [3,4], vascular stent [5] and artificial joint [6]. However, the high level of residual compressive stress that is dominated by the distorted atomic bond structure in DLC films deteriorates the adhesive strength between the film and the substrate, which leads to the failure of coated surface.

Many efforts have been made to reduce the residual stress by controlling the substrate bias during deposition [7], fabricating the multilayer nano-structure [8,9], incorporating third elements into carbon matrix [10,11] and post-annealing process [12]. However, most of the previous works focused on the DLC films with normal incidence of carbon ions, the effect of incident angles on the structure and properties was not given enough attention. Although Liu et al. [13] have revealed that the microscopic structure of the deposited DLC films was influenced seriously by the incident angles of energetic carbon ions, the fundamental understanding of this microstructure and properties evolution from the viewpoint of atomic scale is still unclear due to the limited experimental characterization. Molecular dynamics simulation (MD) has been proved to be an effective method for deeper insight of the atomic bond structure and properties of DLC films in atomic scale. By MD simulation, the variations of structure and properties with the kinetic energy of deposited carbon atoms [14–16], the energy of the carrier gas ions such as Ar^+ [17], hydrogen content [18] or growth species [19,20] have been studied. Joe et al. [21] recently reported the growth of amorphous carbon films by the grazing incidence of energetic carbon atoms and the origin of the rough surface growth under grazing incidences was clarified by the impact-induced uphill transport of the surface atoms. Neyts et al. [22] clarified the influence of the impact angles on the sticking coefficients of several radical species on amorphous carbon surface. But the evolutions of structure and properties with the incident angles are still not fully understood yet.

In the present work, we performed a classical MD simulation to deposit the DLC films with grazing incidence of energetic carbon atoms, the structure and properties evolution were systematically investigated. The dependence of mechanical properties on the incident angles, the distribution of residual stress, the bond length and bond angle distributions were mainly focused. Structural analysis of the films revealed that the grazing incidence of carbon atoms could relax the bond length distortion, which played a key role in the reduction of residual compressive stress.

2. Computational strategy

In order to simulate the deposition of DLC films by MD simulation, the three-body empirical potential Tersoff was chosen to describe the

* Corresponding author at:Division of Surface Engineering, Ningbo Institute of Materials Technology and Engineering, Chinese Academy of Sciences, Ningbo 315201, PR China. Tel.: +86 574 86685170; fax: +86 574 86685159.
E-mail address: aywang@nimte.ac.cn (A. Wang).

0040-6090/$ – see front matter
http://dx.doi.org/10.1016/j.tsf.2013.12.012

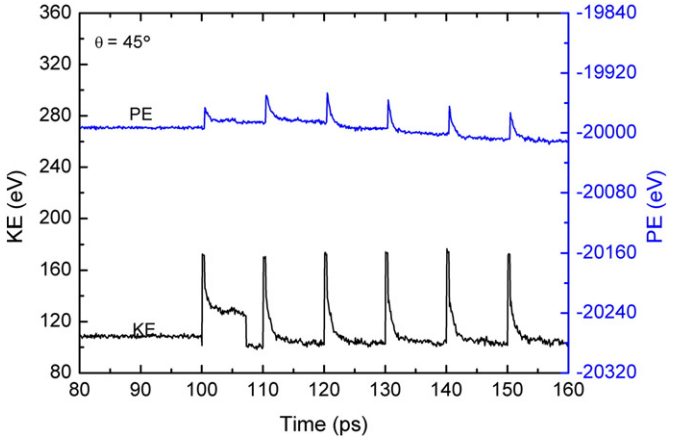

Fig. 1. Energetic variation during the deposition process when the incident angle is 45°.

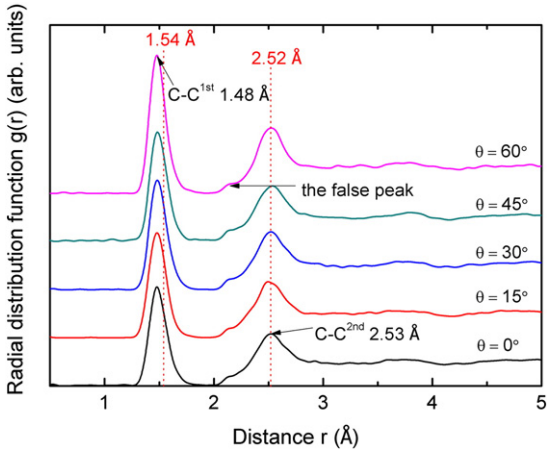

Fig. 3. RDF of DLC films with the different incident angles of carbon atoms.

interaction between the deposited carbon atoms and the diamond substrate [23]. Even if the calculated results have revealed the limit of Tersoff potential where the π bonding is not adequately considered [24–26], it is still demonstrated to be an effective potential for carbon-based system.

The diamond (001) single crystal of 25.2210 × 25.2210 ×24.0758 $Å^3$ in the *x*, *y* and *z* directions was used as substrate, which contained 2800 carbon atoms with 100 atoms per layer and was equilibrated at 300 K for 100 ps before deposition. The incident carbon atoms were introduced at the position of 10 nm above the substrate surface at a random {x, y} position. The positions of atoms in the bottom two layers were frozen to mimic the bulk substrate, while all the other atoms were unconstrained. The kinetic energy of incident carbon atoms was fixed at 70 eV/atom, because it was the optimum energy for a highly stressed and dense DLC film deposition [27]. The impacts of 2000 carbon atoms were simulated and the incident angles of carbon atoms, θ, were varied from 0 to 60°. The periodic boundary conditions were applied in *x* and *y* directions and the time step was fixed at 1 fs.

The time interval between two sequential deposited carbon atoms was 10 ps, which induced an impracticable ion flux of 1.57 × $10^{27}/m^2s$. The changes in kinetic energy (KE) and potential energy (PE) during the deposition process are illustrated in Fig. 1. It indicates that the time interval of 10 ps is enough for relaxing the atomic structure and diminishing the unrealistic effect of high carbon flux on the deposition process. However, it should be noted that a number of processes such as diffusion or rearrangement processes occur on much longer time scales. They are neglected in the simulation due to the required computation time. The substrate temperature was rescaled to 300 K by the Berendsen method [28] after the atomic rearrangement caused by the bombardment of incident atom was finished.

3. Results and discussion

Fig. 2 shows the final morphologies of DLC films at the incident angles of 0–60°, where colors represent the different coordination numbers. All the deposited films show the typical amorphous feature which will be described later by the radial distribution functions (RDF). At the normal incidence (Fig. 2a), the deposited film shows the dense structure with a smooth surface [27]. With the increase of incident angle from 0 to 60°, the surface roughness of DLC films increases and more porous structure is generated, implying the change of mechanical properties. In addition, Fig. 2d–e shows the emergence of a bump-like surface structure, which is in good agreement with the MD calculation results [21]. Because the fixed incident energy of 70 eV/atom is much higher than the cohesive energy of diamond (7.6–7.7 eV/atom), the incident atoms can penetrate into the diamond lattice and intermix with the substrate atoms. Therefore, a significant intermixing layer between the film and the substrate can be observed for each case (Fig. 2).

The RDF spectra of DLC films are shown in Fig. 3, in which the red dotted lines represent the positions of the 1st nearest neighbor (1.54 Å) and the 2nd nearest neighbor (2.52 Å) of crystalline diamond, respectively. First of all, the RDF spectra reveal that all the films are amorphous with the characters of long-range disorder and short-

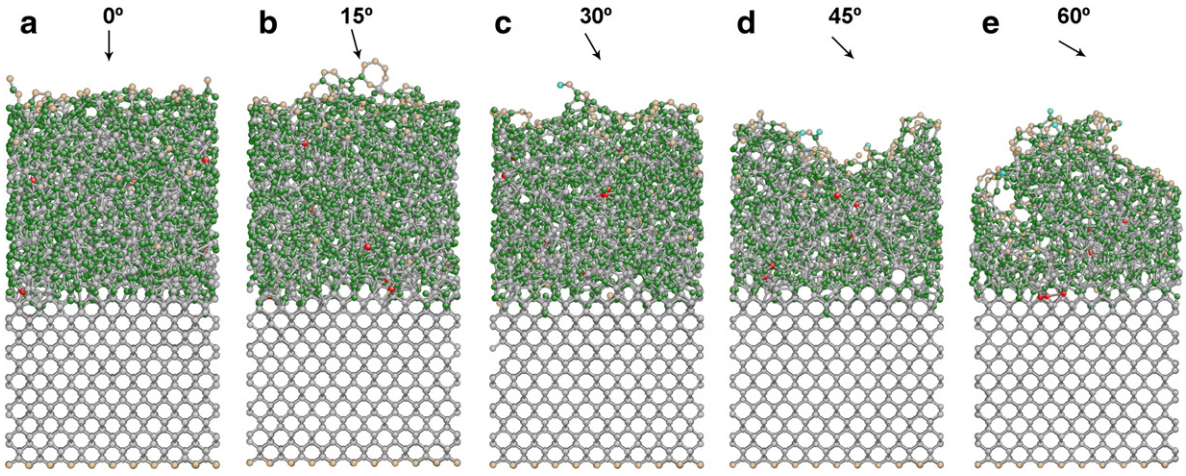

Fig. 2. Snapshots of the films at the incident angles of (a) θ = 0°, (b) θ = 15°, (c) θ = 30°, (d) θ = 45° and (e) θ = 60°, where blue, yellow, green, gray and red colors represent the different coordination numbers of 1, 2, 3, 4 and 5, respectively.

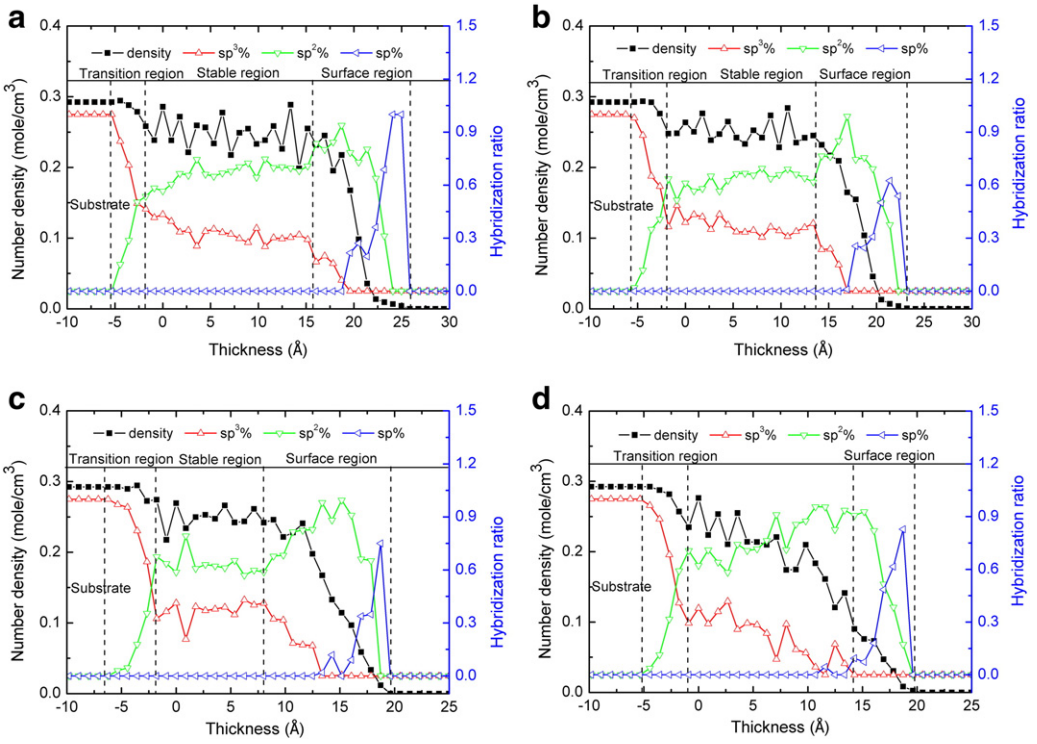

Fig. 4. Variations of number density and hybridization ratio (sp^3%, sp^2% or sp%) along the growth direction at the incident angles of (a) $\theta = 15°$, (b) $\theta = 30°$, (c) $\theta = 45°$ and (d) $\theta = 60°$. The positive direction in horizontal axis corresponds to the films, while the negative direction represents the original substrate.

range order. For all DLC films, the 2nd peak positions are located at 2.53 Å which is similar to that of diamond, while the 1st peak positions observed at 1.48 Å are much smaller than that of diamond. This indicates that the decrease in the C–C bond distance would be one of the major reasons for the high compressive stress of DLC films. Comparing with the DLC film at the normal incidence ($\theta = 0°$), increasing the incident angles makes no contribution to the positions of the 1st and 2nd peaks. At the position of 2.1 Å shown in Fig. 3, the small sharp peak is caused by the cut-off radius of the Tersoff potential, termed as "false peak" [29,30].

Before characterizing the film properties such as density and stress, the variations of properties with film depth were investigated. Fig. 4 shows the variations of number density and hybridization ratio along the film growth direction when the incident angle is 15°, 30°, 45° and 60°, respectively. The characteristic at the incident angle of 0° has been shown in previous work [27]. Fig. 4a–c reveals that the whole system is divided into four regions including substrate, transition region, stable region and surface region, which is similar to the case at 0°. However, it is noted that there is no stable region in the DLC film deposited at the incident angle of 60° (Fig. 4d). Therefore, the whole properties of the films at the incident angle of 0°, 15°, 30° and 45° are quantified in the stable region where the number density and hybridization ratio exhibit a relatively constant value. One should note that the sp^3 fraction in all films appears low values around 33 to 37%, which might attribute to the limit of Tersoff potential where the π bonding was not adequately considered.

Fig. 5 shows the dependence of the number density and residual compressive stress on the incident angles. When the incident angle is 0°, the DLC film owns a high residual compressive stress of about 15.5 GPa [27]. Following the increase of incident angles, the compressive stress increases slightly and then decreases rapidly, while there is no serious change of number density. When the incident angle is 45°, the compressive stress drops to 13.7 GPa and the number density only decreases from 0.250 to 0.247 mole/cm^3. By contrast, the change of

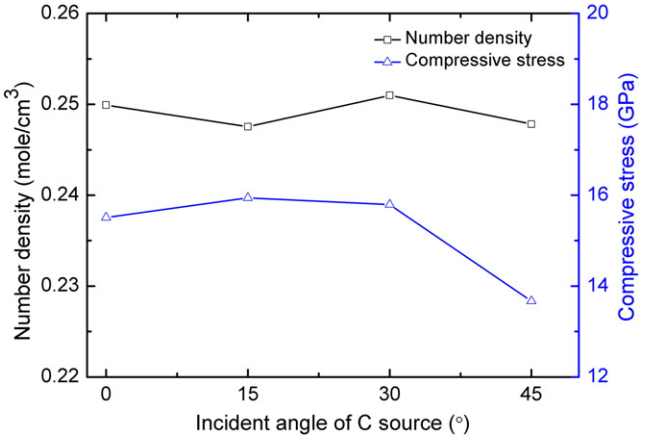

Fig. 5. Evolution of umber density and residual compressive stress as a function of incident angles.

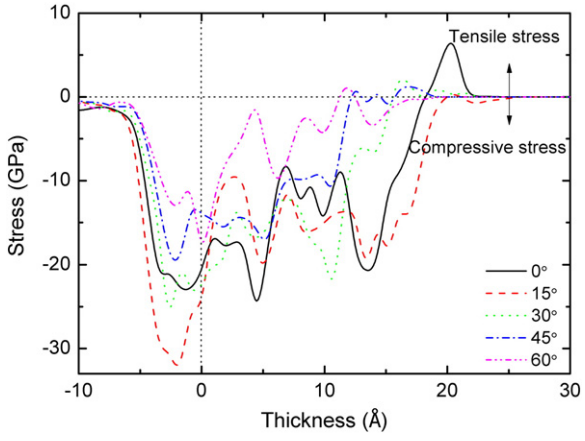

Fig. 6. Stress distribution along the growth direction at the different incident angles.

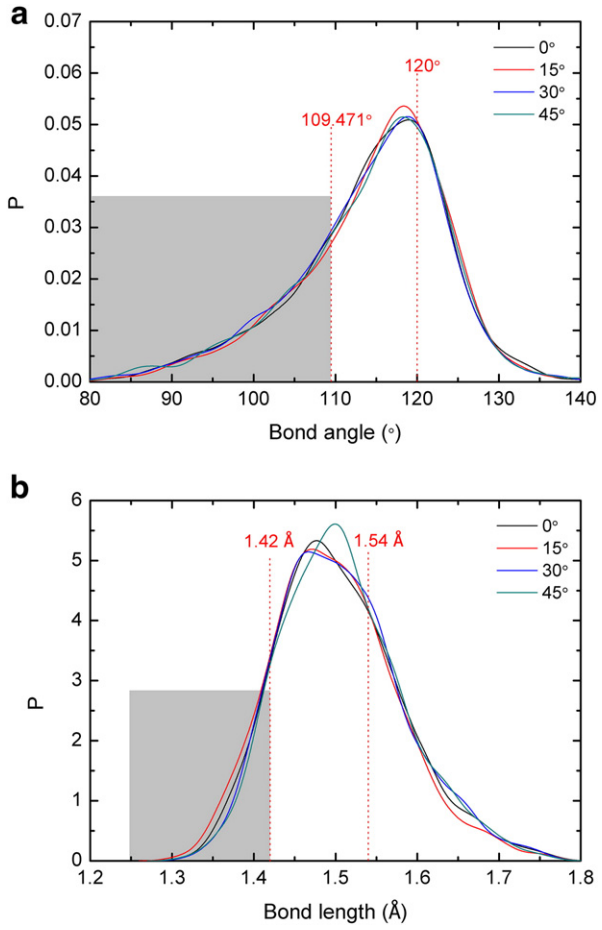

Fig. 7. Bond angles and bond length distribution functions. (a) Bond angle distribution. (b) Bond length distribution.

incident angles results in the residual compressive stress being reduced by 12% without the significant deterioration of the mechanical behavior.

The further analysis of residual stress along the growth direction is demonstrated in Fig. 6. The compressive stress is dominant in all DLC films with different incident angles and the transition region shows higher stress than the stable region or the surface region. Especially, incident angles make more important influence on the stress in the transition region than that in the stable region; following the increase of incident angles, the compressive stress in the transition region increases drastically and then drops.

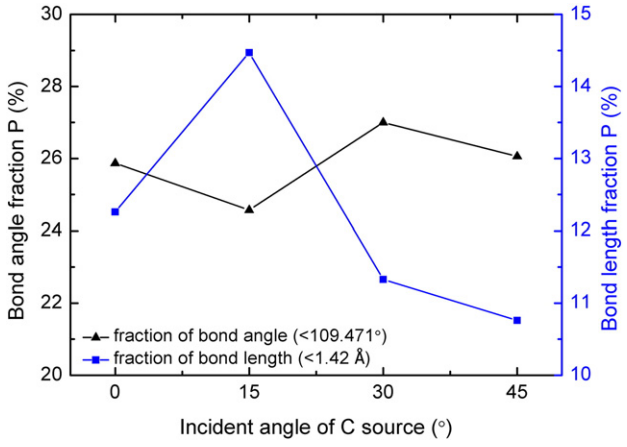

Fig. 8. Bond angle fraction (<109.471°) and bond length fraction (<1.42 Å) integrated from the bond angle distribution and bond length distribution, respectively.

In order to clarify the properties in terms of the atomic bond structure, the bond angles and bond length were analyzed. Fig. 7 shows the bond angles and bond length distributions for DLC films at the incident angle of 0°, 15°, 30° and 45°. The stable bond angle of graphite is 120° and the diamond one is 109.471° (red dot line in Fig. 7a); the stable bond length of graphite is 1.42 Å and the diamond one is 1.54 Å (red dot line in Fig. 7b). It can be found that the bond angle distribution shows a peak at approximately 120°, indicating that the contribution from the threefold coordinated atom is prominent for each case; but the peak position and the peak width are independent of the increase of incident angles (Fig. 7a). Fig.7b shows that the peak position has an obvious shift at the incident angle of 45°, suggesting the change of the bond length. Previous study has revealed that the high compressive stress mainly originated from the distortion of both the bond angles and bond length which were less than 109.471° and 1.42 Å, respectively [27]. As a result, the fractions of bond angles (<109.471°) and bond length (<1.42 Å) are obtained by separately integrating the bond angle distribution and bond length distribution, as illustrated in Fig. 8. These results indicate that the variation of incident angles affects the distorted structure of carbon matrix; when the incident angle is 45°, the reduction of residual compressive stress mainly attributes to the relaxation of distorted C–C bond length.

4. Conclusion

MD simulation was carried out to investigate the effect of incident angles of energetic carbon atoms on the structure and properties of DLC films, in which Tersoff potential was used for C–C interactions. With the increase of incident angles from 0 to 60°, the surface roughness of DLC films increased and more porous structure was generated; except the case of 60°, the whole system was involved in four regions including the substrate, transition region, stable region and surface region. The number density and the compressive stress changed according to the various regions. When the incident angle was 45°, the compressive stress was reduced by 12% with only slight 1.2% decrease of the number density, implying that the residual stress could be decreased significantly without obvious deterioration of mechanical properties by controlling the incident angles. In addition, the stress distribution revealed that the incident angles of carbon atoms had more serious effect on the stress in the transition region than that in the stable region. By further analysis of both the bond angles and bond length distributions, it revealed that the change of incident angles significantly decreased the fraction of distorted bond length in the amorphous carbon matrix, resulting in the reduction of the residual compressive stress.

Acknowledgments

This research was supported by the State Key Project of Fundamental Research of China (2012CB933003, 2013CB632302), the National Natural Science Foundation of China (51371187) and the Ningbo Science and Technology Innovation Team (2011B81001).

References

[1] J. Brand, R. Gadow, A. Killinger, Surf. Coat. Technol. 180–181 (2004) 213.
[2] A.H. Lettington, Carbon 36 (1998) 555.
[3] R. Hauert, Diamond Relat. Mater. 12 (2003) 583.
[4] N. Ali, Y. Kousar, T.I. Okpalugo, V. Singh, M. Pease, A.A. Ogwu, J. Gracio, E. Titus, E.I. Meletis, M.J. Jackson, Thin Solid Films 515 (2006) 59.
[5] P.D. Maguire, J.A. McLaughlin, T.I.T. Okpalugo, P. Lemoine, P. Papakonstantinou, E.T. McAdams, M. Needham, A.A. Ogwu, M. Ball, G.A. Abbas, Diamond Relat. Mater. 14 (2005) 1277.
[6] A.S. Loir, F. Garrelie, C. Donnet, J.L. Subtil, M. Belin, B. Forest, F. Rogemond, P. Laporte, Appl. Surf. Sci. 247 (2005) 225.
[7] D. Sheeja, B.K. Tay, S.P. Lau, X. Shi, Wear 249 (2001) 433.
[8] C. Mathioudakis, P.C. Kelires, Y. Panagiotatos, P. Patsalas, C. Charitidis, S. Logothetidis, Phys. Rev. B 65 (2002) 205203.
[9] L.F. Bonetti, G. Capote, L.V. Santos, E.J. Corat, V.J. Trava-Airoldi, Thin Solid Films 515 (2006) 375.
[10] M. Ban, T. Hasegawa, Surf. Coat. Technol. 162 (2002) 1.

[11] A.Y. Wang, K.R. Lee, J.P. Ahn, J.H. Han, Carbon 44 (2006) 1826.
[12] W. Zhang, A. Tanaka, K. Wazumi, Y. Koga, B.S. Xu, Diamond Relat. Mater. 13 (2004) 2166.
[13] D.P. Liu, G. Benstetter, E. Lodermeier, J. Vancea, J. Vac. Sci. Technol. A 21 (2003) 1665.
[14] B. Zheng, W.T. Zheng, S.S. Yu, H.W. Tian, F.L. Meng, Y.M. Wang, J.Q. Zhu, S.H. Meng, X.D. He, J.C. Han, Carbon 43 (2005) 1976.
[15] E. Neyts, A. Bogaerts, R. Gijbels, J. Benedikt, M.C.M. van de Sanden, Diamond Relat. Mater. 13 (2004) 1873.
[16] B.A. Pailthorpe, J. Appl. Phys. 70 (1991) 543.
[17] E. Neyts, M. Eckert, A. Bogaerts, Chem. Vap. Depos. 13 (2007) 312.
[18] E. Neyts, A. Bogaerts, M.C.M. van de Sanden, Appl. Phys. Lett. 88 (2006) 141922.
[19] E. Neyts, A. Bogaerts, M.C.M. van de Sanden, J. Appl. Phys. 99 (2006) 014902.
[20] E. Neyts, M. Tacq, A. Bogaerts, Diamond Relat. Mater. 15 (2006) 1663.
[21] M. Joe, M.W. Moon, J. Oh, K.H. Lee, K.R. Lee, Carbon 50 (2012) 404.
[22] E. Neyts, A. Bogaerts, Phys. Chem. Chem. Phys. 8 (2006) 2066.
[23] J. Tersoff, Phys. Rev. Lett. 61 (1988) 2879.
[24] N. Marks, J. Phys. Condens. Matter 14 (2002) 2901.
[25] S.H. Lee, C.S. Lee, S.C. Lee, K.H. Lee, K.R. Lee, Surf. Coat. Technol. 177–178 (2004) 812.
[26] H.U. Jäger, A.Yu. Belov, Phys. Rev. B 68 (2003) 024201(1).
[27] X. Li, P. Ke, H. Zheng, A. Wang, Appl. Surf. Sci. 273 (2013) 670.
[28] H.J.C. Berendsen, J.P.M. Postma, W.F. van Gunsteren, A. DiNola, J.R. Haak, J. Chem. Phys. 81 (1984) 3684.
[29] T.B. Ma, Y.Z. Hu, H. Wang, Acta Phys. Sin. 55 (2006) 2922.
[30] N.A. Marks, Diamond Relat. Mater. 14 (2005) 1223.